TEMPORAL AND SPATIAL VARIABILITY IN METEOSAT/SEVIRI IMAGES FOR THE GLOBAL SPACE-BASED INTER-CALIBRATION SYSTEM (GSICS)

Tim Hewison

EUMETSAT

ABSTRACT

Inter-calibration of satellite instruments often require comparing observations from different instruments collocated in space, time and viewing geometry within certain thresholds. The choice of these thresholds directly impacts the uncertainty of the comparison, partially due to the scene variability within the range of the collocation criteria. Scene variability can be quantified as variograms by evaluating the root mean square difference of a series of observations sampled at different intervals in space or time. These are evaluated here using data from the infrared channels of the Meteosat/SEVIRI geostationary imager. The results suggest thresholds of 5 min and 3.5 km would each introduce random uncertainties of about 1-2 K into each collocation.

Index Terms—Calibration, Earth Observing System, Infrared image sensors, Measurement uncertainty, Meteorology

1. INTRODUCTION TO GSICS

The Global Space-based Inter-Calibration System (GSICS) [1] is an international collaborative effort which aims to monitor, improve and harmonize the quality of observations from operational weather and environmental satellites of the Global Observing System (GOS). GSICS aims at ensuring consistent accuracy among space-based observations worldwide for climate monitoring, weather forecasting, and environmental applications. This is achieved through a comprehensive calibration strategy, which involves monitoring instrument performances, operational inter-calibration of satellite instruments, tying the measurements to absolute references and standards, and recalibration of archived data. A major part of this strategy involves direct comparison of collocated observations from pairs of satellite instruments, which are used to systematically generate calibration functions to compare and correct the calibration of *monitored* instruments to references. These *GSICS Corrections* are needed for accurately integrating data from multiple observing systems into both near real-time and re-analysis products, applications and services.

2. UNCERTAINTY ANALYSIS OF GSICS PRODUCTS

GSICS procedures are built on the principle of traceability to common references through an unbroken chain of comparisons, each with specified uncertainty. The specification of this uncertainty is achieved by constructing an error budget, considering each process in the inter-calibration algorithm and evaluating the uncertainties on key variables due to random and systematic effects [2] and the sensitivity of the GSICS Corrections to these.

Inter-calibration of satellite instruments often require comparing observations from different instruments coincident in space, time and viewing geometry. As these collocations are rarely exact, thresholds are usually applied to define the collocations. The choice of these thresholds directly impacts the uncertainty of the comparison, partially due to the scene variability within the range of the collocation criteria, which themselves represent trade-offs between the errors on each collocation and the number of collocations available.

Scene variability can be quantified as a variogram by evaluating the root mean square difference of a series of observations sampled at different intervals in space or time [3]. Variograms are also known as empirical semi-variances and are similar to the concept of Structure Functions in meteorology [4] and Allan Variance [5]. They allow the variability of stochastic processes to be quantified over specific spatial or temporal scales and can quantify errors of representativeness in the use of satellite data. These are evaluated here using data from the infrared channels of the Meteosat/SEVIRI geostationary imager.

3. TEMPORAL VARIABILITY

The temporal variogram, $2\gamma_t(\Delta t)$ is calculated between brightness temperatures, $T_b s$, sampled at different intervals, Δt, from an extended time-series, $T_b(t)$:

$$2\hat{\gamma}_t(\Delta t) := \frac{1}{n_i n_j n_k} \sum_{i,j,k} \left[T_b\left(x_i, y_j, t_k + \Delta t\right) - T_b\left(x_i, y_j, t_k\right) \right]^2 \quad (1)$$

where x_i, y_j are longitude and latitude over the SEVIRI grid and t_k represents a time series of SEVIRI images.

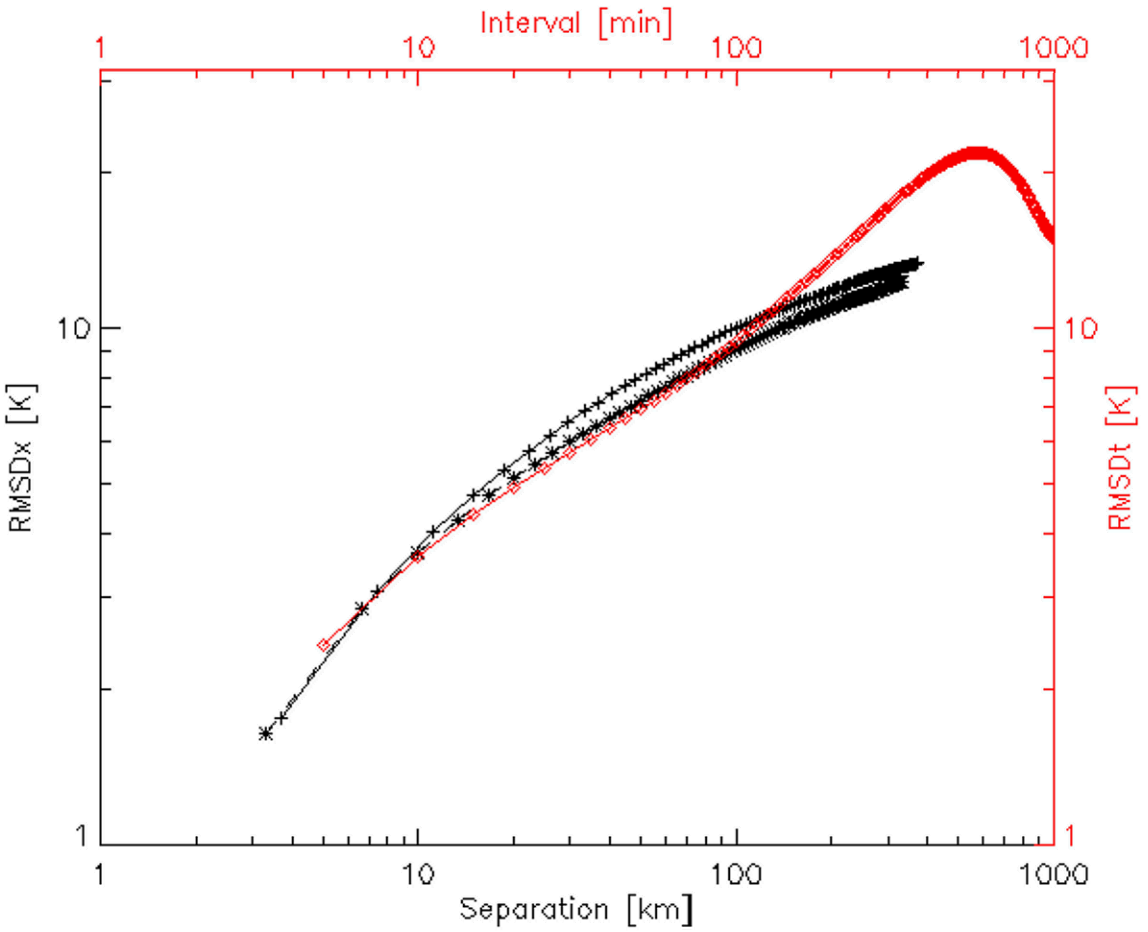

Figure 1: Variograms calculated as rms differences in Meteosat-8/SEVIRI 10.8 µm brightness temperatures with time intervals from Rapid Scanning Meteosat data (red diamonds, upper x-axis) and with spatial separation in North-South direction (black pluses, lower x-axis) and West-East direction (black stars, lower x-axis).

Here, the T_b variability is estimated from observations from the infrared channels of the Meteosat-8/SEVIRI imager, which provides data sampled every 3 km at nadir and every 15 min in normal operations over the full Earth disc (or every 5 min over a limited area). The red curve in Figure 1 shows $2\gamma_t(\Delta t)$ for the 10.8 µm channel on temporal scales of 5 min to 16 hr.

The temporal T_b variability was calculated from a series of observations made in rapid scanning mode on 2008-04-18 sampling the area 15°N 30°W-30°E, 45°N 45°W-45°E, every 5 min over a 24 hr period. The results are similar to those calculated from a larger area (within 30° lat/lon of the sub-satellite point) scanned every 15 min over another 24 hr period (2006-02-04).

The temporal variogram, shown as the red curve in Figure 1, shows the temporal variability peaks at Δt ~12 hr, corresponding to the diurnal cycle. This is common to all channels, but most pronounced in the window channels. It is apparent that the diurnal cycle dominates variability on time scales longer than ~1 hr, causing γ_t to increase more rapidly for increasing time intervals.

4. SPATIAL VARIABILITY

The spatial Tb variability was calculated over the area within 30° lat/lon of the sub-satellite point from data obtained at 2006-02-01 01:00 UTC. The image in each channel was shifted by variable distances, Δx, and the spatial variogram, γ_x, was calculated for each as:

$$2\hat{\gamma}_x(\Delta x) := \frac{1}{n_i n_j n_k} \sum_{i,j,k} \left[T_b\left(x_i + \Delta x, y_j, t_k\right) - T_b\left(x_i, y_j, t_k\right) \right]^2 \quad (2)$$

As expected, the black curves in Figure 1 show γ_x increases with increasing spatial separation at scales of 3 to 1000 km. There is more T_b variability in the N/S direction than E/W because of the global latitudinal temperature

gradient. However, this difference becomes negligible on scales smaller than ~10 km.

5. MATCHING SPATIAL AND TEMPORAL COLLOCATION CRITERIA

This method allows the scene variability to be quantified for observations sampled at any interval in space or time. For example, Table 1 shows the spatial and temporal variograms evaluated as the r.m.s. difference in scene T_bs sampled every 3.5 km and 5 min, respectively. For all channels, $\gamma_t(\Delta t=5\text{min})$ and $\gamma_x(\Delta x=3.5\text{km})$ were found to produce similar variances. Therefore, the random component of uncertainty in each collocation due to scene variability can be estimated by scaling the observed spatial variability alone by a factor of $\sim\sqrt{2}$.

In Table 1 the window channels show most variability on these scales, because they are most sensitive to clouds, while the channels more sensitive to atmospheric absorption show least variability.

Table 1: Temporal and spatial variograms evaluated as RMS difference of Meteosat-8 brightness temperatures on scales of 5 min and 3.5 km, respectively.

Channel [μm]	$\{2\gamma_t(\Delta t=5\text{min})\}^{1/2}$ [K]	$\{2\gamma_x(\Delta x=3.5\text{km})\}^{1/2}$ [K]
3.9	1.7	2.1
6.2	0.4	0.5
7.3	0.8	0.8
8.7	1.7	1.6
9.7	0.9	1.2
10.8	1.8	1.7
12.0	1.8	1.6
13.4	1.2	1.2

6. FILTERING

A homogeneity filter can be applied by excluding pixels where the standard deviation of radiances within 5x5 pixels are >5% of the mean radiance. When this is applied prior to the calculation, γ_t drops by a factor of 2.0 and γ_x reduces by a factor of 2.6. Selecting only clear sky cases will further reduce both γ_t and γ_x. On very small scales, or for homogeneous scenes, the atmospheric variability becomes negligible compared to the instrument's radiometric noise and γ_x and γ_t become constant with space and time, respectively.

7. CONCLUSIONS

In this study, optimization of collocation thresholds are found to depend on how much noise is acceptable to introduce into each collocation due to scene variability. For example, these results suggest thresholds of 5 min and 3.5 km would each introduce random uncertainties of about 1-2 K into each collocation. These may be reduced to insignificant levels if many independent collocations are combined in the analysis. However, adjacent collocations are highly correlated (autocorrelation 1/e scales are about 600 km and 6 hr), so it is not trivial to optimize the collocation thresholds from this analysis alone.

8. REFERENCES

[1] Goldberg, M., G. Ohring, J. Butler, C. Cao, R. Datla, D. Doelling, V. Gaertner, T. Hewison, B. Iacovazzi, D. Kim, T. Kurino, J. Lafeuille, P. Minnis, D. Renaut, J. Schmetz, D. Tobin, L. Wang, F. Weng, X. Wu, F. Yu, P. Zhang and T. Zhu, "The Global Space-based Inter-Calibration System (GSICS)", *Bulletin Am. Meteorol. Soc*, doi:10.1175/2010BAMS2967.1, 2011.

[2] Hewison, T., 2011, "GSICS SEVIRI-IASI Inter-calibration Uncertainty Evaluation", *Proceedings of 2011 EUMETSAT Meteorological Satellite Conference*, Oslo, Norway 5 - 9 September 2011, EUMETSAT P.59, ISBN 978-92-9110-093-4, ISSN 1011-3932, 2011.

[3] Cressie, N., Statistics for spatial data, Wiley Interscience, 1993.

[4] Allan, D.W., "Statistics of Atomic Frequency Standard", *Proc IEEE*, 54, No.2, pp.221-231, 1996.

[5] Kitchen, M., "Representativeness errors for radiosonde observations", *Q.J.R. Meteorol. Soc.*, Vol.115, pp.673-700, 1989.